

Large-Scale Development of Antibacterial Scaffolds: Gentamicin Sulfate-Loaded Biodegradable Nanofibers for Gastrointestinal Applications

Marketa Klicova,* Senta Mullerova, Jachym Rosendorf, Andrea Klapstova, Radek Jirkovec, Jakub Erben, Michaela Petrzelkova, Hedvika Raabová, Dalibor Šatinský, Jana Melicherikova, Richard Palek, Vaclav Liska, and Jana Horakova



Cite This: *ACS Omega* 2023, 8, 40823–40835



Read Online

ACCESS |

Metrics & More

Article Recommendations

ABSTRACT: The ever-increasing demands of modern medicine drive the development of novel drug delivery materials. In particular, nanofibers are promising for such materials due to their favorable properties. However, most development is still carried out through laboratory techniques that do not allow extensive and reproducible characterization of materials, which slows medical research. In this work, we focus on the large-scale fabrication and testing of specific antibacterial nanofibrous materials to prevent the postoperative complications associated with the occurrence of bacterial infection. Poly- ϵ -caprolactone with gentamicin sulfate (antibiotic) in different concentrations was electrospun via a needless device. The amount of antibiotics was proven by elemental analysis, UV spectrophotometry, and HPLC. The cytocompatibility of the materials was verified in vitro according to ISO 10993-5. The cell adhesion and proliferation were assessed after 2, 7, 14, and 21 days using the CCK-8 metabolic assay, fluorescence, and scanning electron microscopy. The tested nanofiber materials supported cell growth. Antibacterial tests were performed to confirm the release of gentamicin sulfate, and its antibacterial properties were proven toward *Staphylococcus gallinarum* and *Escherichia coli* bacteria. The effect of ethylene oxide sterilization was also studied. The sterilized nanofibrous layers are cytocompatible while antibacterial and therefore suitable for medical applications.

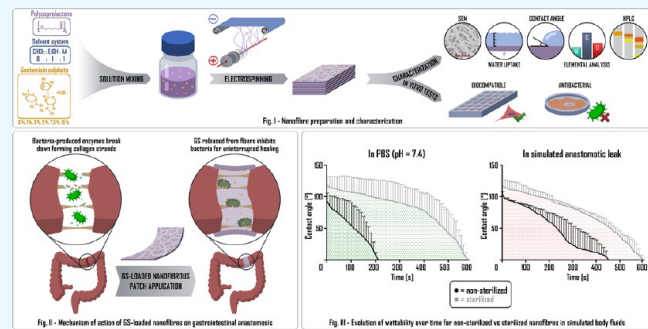


Fig. I - Nanofiber preparation and characterization

Fig. II - Mechanism of action of GS-loaded nanofibers on gastrointestinal ulceration

Fig. III - Evolution of viability over time for non-sterilized vs sterilized nanofibers in simulated body fluids

In PBS (pH = 7.4)

In simulated gastrointestinal leak

1. INTRODUCTION

Drug delivery systems based on nanofibers are meeting the ever-increasing demands of modern medicine due to their ability to maintain consistent absorption while decreasing systemic side effects, minimizing the frequency of dosing, and other indisputable benefits.¹ The use of certain antibiotics orally or intravenously increases the risk of intestinal microbiome deterioration and possible systemic side effects. Such a disbalance causes mainly diarrhea, which is especially dangerous in the early postoperative period. The development of drug delivery structures with incorporated antibiotics is also of key importance due to growing antibiotic resistance. It was predicted that in the year 2050, antibiotic resistance could cause around 50 million deaths annually.¹ There have been many attempts to develop efficient drug delivery tools in recent years, including systems such as nanoparticles, micelles, liposomes, etc.²

Nanofibrous materials are favorable due to their large surface area, porosity, and desirable properties for medicine such as similarity to the native extracellular matrix, biocompatibility,

and controlled biodegradability.^{1,3} There are several available methods for the preparation of nanofibrous mats. In particular, a technique called electrospinning is the most commonly used one for fabrication of nano- to microsized fibers due to the low cost and flexibility of the process.¹

Several research articles have previously reported the use of nanofibrous materials as antibiotic delivery drug systems. Pisani et al. incorporated the antibiotic gentamicin sulfate (GS) in a concentration of 1% w/w into polylactide (PLA)/ polycaprolactone (PCL) copolymer nanofiber layers. The polymer solution with the antibiotic was electrospun via laboratory needle equipment.⁴ In a study by Yang et al., the GS antibiotic was incorporated into PCL nanofiber layers.

Received: August 11, 2023

Accepted: September 29, 2023

Published: October 17, 2023



Antibiotic concentrations were 0, 2.5, 5, and 10% w/w. The materials were prepared by needle electrospinning in different thicknesses.⁵ The study by Sirc et al. describes the production and release of incorporated antibiotic GS from a three-layer nanofibrous material made of poly(vinyl alcohol) (PVA) and polyurethane (PU).⁶ Publication by Coimbra et al. examines the differences between GS-enhanced biodegradable nanofibers produced by suspension and emulsion electrospinning.⁷ Abdul Khodir et al. reported on development of needle electrospun nanofibrous layers based on PCL and collagen with the antibiotic GS for healing of skin infections.⁸

As was stated in the previous paragraph, several research articles were already published to describe the behavior of nanofibrous drug delivery systems. However, most of them were prepared using the technique of needle electrospinning, a laboratory equipment-based approach that does not offer sufficient scalability for industrial-scale nanofiber production. Although nanofibrous drug delivery systems are receiving increasing attention, only very few studies describe the production of nanofibers by electrospinning on a semi-industrial scale. The same applies for the lack of data regarding final material properties after sterilization, with only a few studies monitoring the effect of sterilization methods on the resulting nanofibrous structures. This represents an important missing piece of information since the final implanted materials always undergo sterilization. We believe that the lack of these findings leads to the impossibility of transferring the scientific outcomes to industrial and clinical practice.

In this study, we have developed a nanofibrous material based on the biodegradable polycaprolactone (PCL) with an incorporated antibiotic gentamicin sulfate (GS) for a specific biomedical application. Based on our previous research, biodegradable nanofibrous layers could act as barrier materials in gastrointestinal surgery. The planar nanofibers may be applied around the intestinal tissue after surgery (around the gastrointestinal anastomoses). The motivation behind this approach is to minimize the life-threatening postoperative complications that frequently occur following abdominal surgeries. As shown in our previous studies, the nanofibrous patches based on PCL are easy to manipulate during *in vivo* animal studies.^{9–11} Moreover, the nanofibrous layers are convenient for surgeons; they easily adhere to the tissue without prolonging the operation time and can be used *in situ* as the drug's matrices. We previously evaluated the PCL nanofibers; however, we believe that by directly enhancing the nanofibrous structures with active substances, it is possible to provide valuable improvements in many biomedical applications. This is based on the assumption that influencing the intestinal bacteria or preventing an increase in the collagenolytic activity of the healing anastomosis can significantly reduce the incidence of anastomotic leak in colorectal surgery. However, we would like to remark that the presented findings are usable for many other applications as well, such as use of nanofibrous drug delivery systems for antibacterial wound healing and other procedures.

In the following sections, we report large-scale production and evaluations of the PCL nanofibers with GS before and after the sterilization process. The nanofibrous layers were produced via a needleless electrospinning device, the structure was observed via scanning electron microscopy, and the presence of the antibiotic was confirmed by using high-performance liquid chromatography (HPLC). The antibacterial properties were tested with two strains: *Escherichia coli* (*E.*

coli) and *Staphylococcus gallinarum* (*S. gallinarum*). The *in vitro* testing with animal cells proved the cytocompatibility of the developed drug delivery systems.

2. MATERIALS AND METHODS

2.1. Polymeric Solutions. A total of six polymer solutions were prepared from a PCL granulate (M_w , 45,000 g/mol, Sigma-Aldrich, USA) with a concentration of 16% w/w PCL in the solvent system chloroform/ethanol/acetic acid (Penta Chemicals, CZE) with a ratio of 8/1/1 v/v/v. Antibiotic concentrations of GS (Sigma-Aldrich, USA) in the PCL solutions were 0, 1, 3, 5, 7.5, and 10% w/w. The antibiotic concentration was calculated from the dry weight of the PCL granulate. The solutions without an antibiotic content were stirred for 24 h, and the GS was weighed and added directly before electrospinning to prevent any degradation. The homogeneous distribution of the GS active substance in the solution was ensured by using an ultrasonic sonotrode prior to electrospinning.

2.2. Electrospinning. The prepared polymeric solutions were electrospun via a Nanospider NS 1WSS00U device (Elmarco, CZE), shown in the schematic in Figure 1.

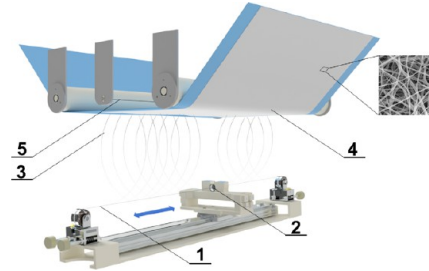


Figure 1. Scheme of the needleless Nanospider electrospinning device: 1, the positive electrode in the form of a steel wire; 2, steel orifice with a polymer solution reservoir; 3, fiber/droplet formation and evaporation of the solvent; 4, nanofibrous layer collected on a supporting textile material; 5, steel wire serving as the negative electrode.

Environmental conditions of the process were controlled by an NS AC150 air conditioner (Elmarco, CZE). The polymer solution was applied from the reservoir to the spinning electrode (a steel wire). The nanofibrous layers were electrospun onto a spunbond (a nonwoven fabric made of polypropylene). The parameters were optimized to obtain a nanofibrous layer with a surface weight of $1 \times 10 \text{ g/m}^2$. The final conditions after optimization are listed in Table 1.

2.3. Sterilization. The prepared materials were sterilized using ethylene oxide (Anprolene, UK) for 12 h at 37 °C. Sterilization was carried out according to the standard ISO 11135-1 (Sterilization of health care products—Sterilization with ethylene oxide—Part 1: Requirements for the development, validation, and continuous control of the sterilization procedure for medical devices). After sterilization, the materials were aerated for 1 week at room temperature.

2.4. Morphology. The samples were observed using a scanning electron microscope (SEM) TESCAN VEGA 3 SB Easy Probe (TESCAN, CZE) at various magnifications for morphological evaluation. Fiber diameters were measured using the ImageJ program (500 values from the images with 5000× magnification).

Table 1. Optimized Process Parameters of Large-Scale Electrospinning via the Nanospider

polymeric solution	PCL	PCL/1%GS	PCL/3%GS	PCL/5%GS	PCL/7.5%GS	PCL/10%GS
rewinding speed [mm/min]	70	65	45	45	40	15
distance between the electrodes [mm]	170	170	170	170	170	170
high voltage [kV]	+40/-10	+40/-10	+40/-10	+40/-10	+40/-10	+40/-10
cartridge movement speed [mm/s]	550	550	550	550	550	550
steel wire movement [mm/min]	15	15	15	15	15	15
temperature [°C]	22 °C	22 °C	22 °C	22 °C	22 °C	22 °C
relative humidity [%]	52%	52%	52%	52%	52%	52%

2.5. Antibiotic Presence and Concentration. Characteristic elements for the GS molecule that do not occur in the PCL chain were analyzed (namely, sulfur and nitrogen). For elemental analysis, two samples were prepared from different areas of the evaluated materials. The prepared samples were placed in aluminum foil with dimensions of 4 × 11 mm and weighed so that the weight of the material was 5 mg. Subsequently, the nanofibers with aluminum foil were reweighed. The standard was sulfanilamide, and the control was pure aluminum foil. The measurement was carried out on an Elementar Vario Cube device with a thermal conductivity detector (TCD) for 90 s at 1200 °C. Both nonsterile and sterile materials were tested.

For the determination of the antibiotic GS concentration in nanofibrous materials using UV spectrophotometry and high-performance liquid chromatography (HPLC), a GS stock solution (Sigma-Aldrich, USA) was prepared with 1 mg of GS in 1 mL of PBS and a ninhydrin solution (NIN, Sigma-Aldrich, USA) with 0.1 g of NIN in 20 mL of PBS. From the nanofibrous materials, samples weighing 5 to 75 mg (depending on the material) were weighed, placed in test tubes, and filled with 2.5 mL of PBS. The composition of PBS was as follows: 8 g of NaCl + 200 mg of KCl + 1.44 g of Na₂HPO₄ + 24.5 mg of KH₂PO₄ were dissolved in 1000 mL of distilled water. Calibration solutions were prepared from GS stock solution in tubes with concentrations of 0.075, 0.1, and 0.15 mg/mL and a volume of 2.5 mL. A blank sample of 2.5 mL of PBS and 2.5 mL of NIN solution was prepared for UV spectrophotometry.

All samples (including blank samples and calibration solutions) were heated for 15 min at 95 °C, and 2.5 mL of NIN solution was added to all samples before heating. The GS-coated nanofiber sheets of approximately 30 × 30 mm size were dissolved during the heating and derivatization procedure, and thus, the GS was released. After the derivatization procedure, a violet-colored gentamicin–ninhydrin complex with an absorption maximum at a wavelength of 570 nm was formed. After heating, the samples were cooled under running water for 1 min. The nanofiber samples were filtered through 0.22 μm polytetrafluoroethylene (PTFE) filter paper before HPLC analysis. Absorption of all samples was measured at a wavelength of 570 nm. Calibration samples were analyzed immediately.

2.5.1. UV Spectrophotometry. Using a blank sample, a zero value at a wavelength of 570 nm was set on a DLAB SP-V1000 spectrophotometer. The intensity of violet coloration of the gentamicin–ninhydrin complex was measured. By measurement of the calibration solutions, the equation of the calibration line was obtained, and the linearity was verified. GS concentrations from nanofiber samples were calculated according to the equation of the calibration line.

2.5.2. HPLC. Standard solutions and coated nanofibers were derivatized before HPLC analysis according to the reported procedure. Measurements were performed on a Shimadzu LC-10 AD chromatograph. From each sample, a volume of 20 μL was injected onto an Ascentis Express ES-CN, 100 × 4.6 mm, 5 μm core–shell particle size analytical column. The mobile phase consisted of acetonitrile (can gradient grade purity, Thermo Fisher, France) and DIW, and their ratio was mixed in a gradient elution. At the beginning of the analysis, ACN:DIW was in a ratio of 5:95 (v/v) to 100:0 (v/v) in the third minute and returned to the initial conditions in 1 min 5:95 (v/v). Before each analysis, the column was equilibrated for 1 min. Each sample was injected in triplicate. The calibration solutions were used in the concentration range from 0.075 to 0.3 mg mL⁻¹ to verify the linearity and the equation of linear regression and to evaluate the concentration of the tested samples. The results of the GS concentration in the nanofibrous material were calculated from the peak areas of chromatograms and the equation of linear regression. Peak areas of GS were evaluated by using Shimadzu LabSolution software at a wavelength of 570 nm.

2.6. Contact Angle. The contact angles were determined via a sessile drop technique using a goniometer See System 6.2 (Advex Instruments, CZE). The liquid drop (5 μL) of distilled water (DIW) was dosed on the surface of both sterile and nonsterile fibrous mats (*n* = 5). An image of the droplet was captured using a CCD camera. The behavior of the drop on the surface of the material was monitored over time until complete absorption was achieved. Continuous values were recorded (every second or every 5 or 10 s). The data were plotted, and the times for complete absorption of the drop for different materials were also compared.

2.7. Absorption. The methodology of liquid absorption into nanofibrous layers was determined based on the publication of Choi et al.¹² The individual samples (20 × 20 mm, *n* = 10) were weighed, the weight was noted (*m*₁), and the individual samples were placed in 10 mL test tubes. Subsequently, the testing liquids, namely, DIW, phosphate buffer saline (PBS), and simulated intestinal fluid (AL, pH = 6.8; Biochemazone, Canada) were separately added to the samples. The samples were left in the fluids for 24 h at 37 °C. After 24 h, the samples were taken out of the tubes and weighed (*m*₂). The wet samples were left to dry at room temperature for 24 h and then weighed again (*m*₃).

The percentage absorption of materials was calculated according to the formula

$$A[\%] = \frac{m_2 - m_1}{m_1} \cdot 100 \quad (1)$$

The percentage weight loss was calculated according to the formula

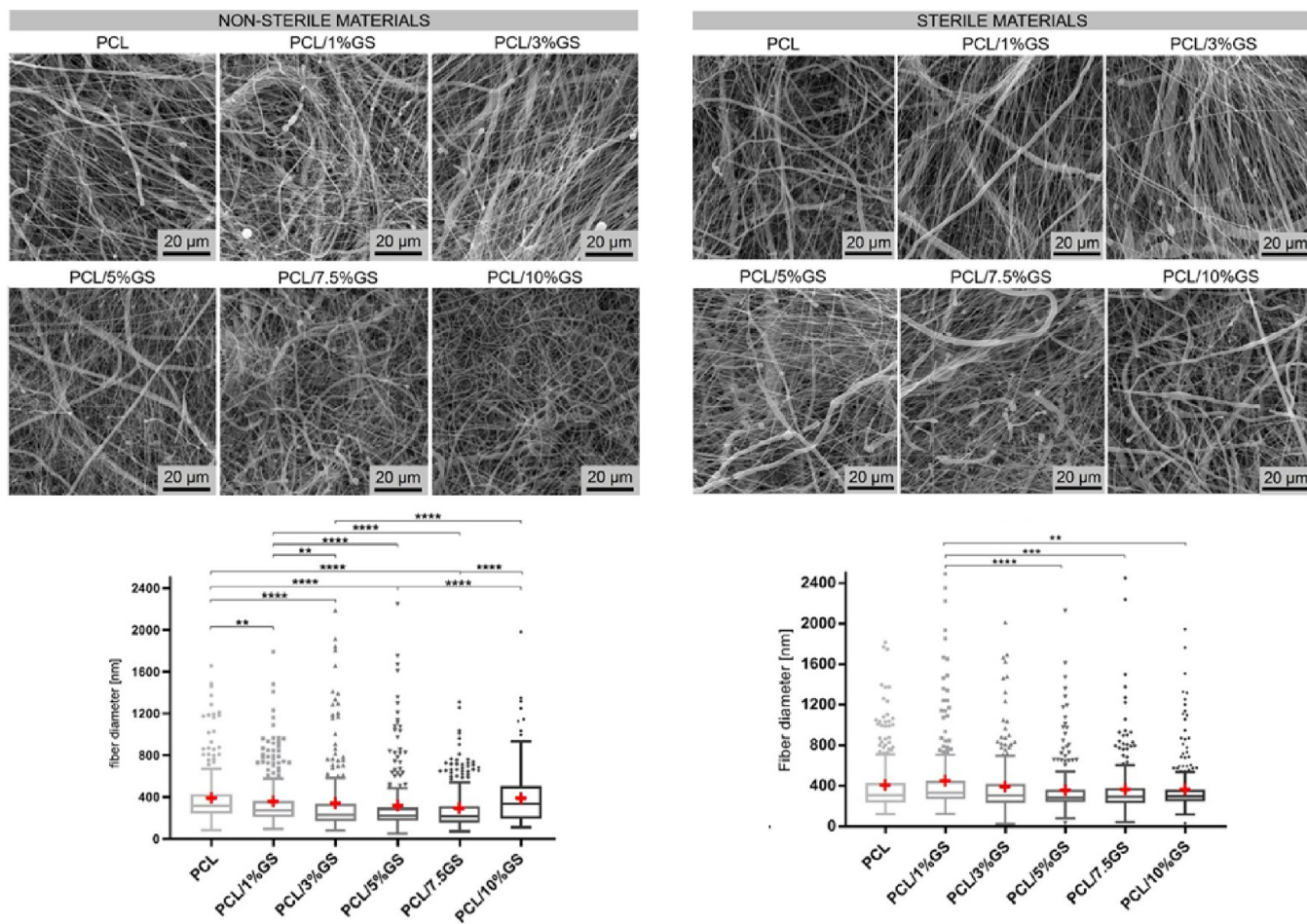


Figure 2. SEM images of the developed materials, with a scale bar of 20 μm , together with nonsterile (left) and sterile (right) materials' diameters ($n = 500$).

$$U[\%] = \frac{m_1 - m_3}{m_3} \cdot 100 \quad (2)$$

where m_{11} is the weight of the dry sample before testing (day 1), m_{12} is the weight of the sample after 24 h in liquid (day 2), and m_{13} is the weight of the sample after complete drying (day 3).

2.8. In Vitro Testing with Animal Cells. Cytotoxicity of material extracts and various concentrations of GS in cell media was performed according to the standard ČSN EN ISO 10993-5 (Biological evaluation of medical devices, Part 5: Cytotoxicity tests in vitro). Materials (10 mg of material per 1 mL of cell medium) were prepared into 15 mL tubes and sterilized with ethylene oxide (Aprolene, UK) for 12 h followed by aeration for 1 week. The concentration series of GS were prepared, namely, 1, 5, 10, 15, 20, 40, 60, 80, 100, and 250 mg of GS in 1 mL of medium (DMEM, Dulbecco's modified Eagle medium, Biosera, France). The material's extracts and the concentration series of GS in DMEM were shaken for 24 h (60 rpm, 37 °C). The prepared extracts and concentration series were added to the confluent layer of 3T3 mouse fibroblast cells (ATCC, USA) in 96-well plates. After 24 h of incubation at 37 °C, the MTT metabolic assay was performed at 570 nm ($\lambda_{\text{reference}}$ was 690 nm).

Cell adhesion and proliferation were tested with 3T3 fibroblasts (ATCC, USA) at a concentration of 7×10^3 cells/well. The metabolic activity of the cells was evaluated

after 4, 7, 14, and 21 days of cultivation by the CCK-8 assay. The cells were also visualized via fluorescence microscopy and SEM.

2.8.1. Metabolic Activity. A 1 mL aliquot of 10% CCK-8 in DMEM medium was added to the cell-seeded materials. Subsequently, the materials were incubated for 3 h in an incubator (37 °C, 5% CO₂). After incubation, 200 μL of the resulting solutions was pipetted into a new 96-well plate. The absorbance at 450 nm was then measured using a spectrophotometer, and the viability, which corresponds to the measured absorbance, was evaluated.

2.8.2. Fluorescence Microscopy. For fluorescence analyses, phalloidin–FITC and DAPI were added to the fixed samples to visualize cells. Cells were captured by a Nikon Eclipse-Ti-E fluorescence microscope (Nikon Imaging, CZE), and the number of cells was quantified by MATLAB software (MathWorks, USA).

2.9. Antibacterial Properties. Antibacterial testing was based on the standard AATCC test method (147-2004 Antibacterial Activity Assessment of Textile Materials: Parallel Streak Method). However, the methodology was modified to meet the needs of testing. Four samples of each material with dimensions of 10 × 40 mm were prepared for the experiment. Samples were removed from the supporting textile (spunbond) before testing. The tested bacterial cultures were *Escherichia coli* CCM 7929 (Gram-negative) and *Staphylococcus gallinarum* CCM 3572 (Gram-positive). Petri dishes with TBX (Tryptone

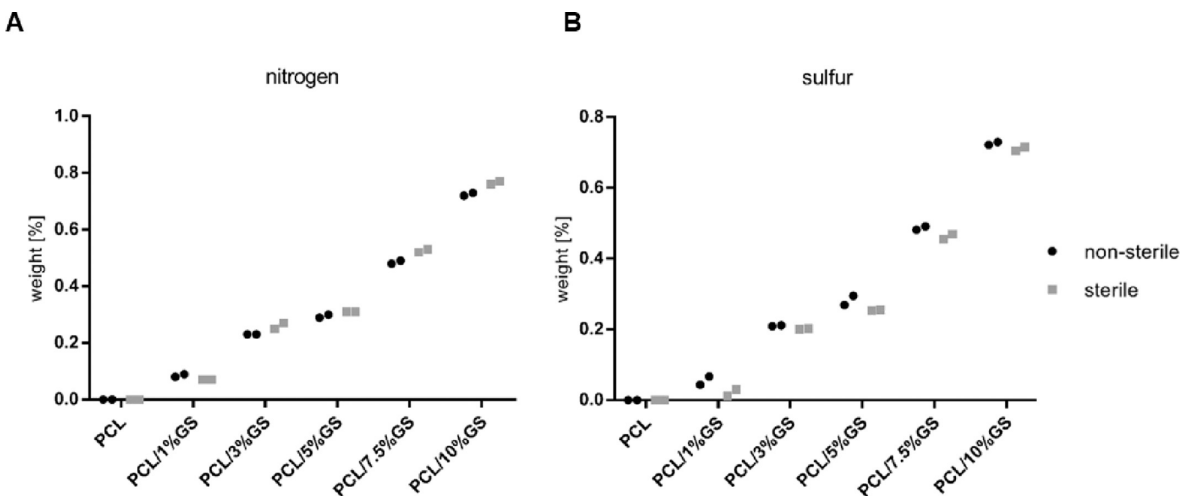


Figure 3. Elemental analysis of PCL nanofibers with different concentrations of GS. Measuring the amount of nitrogen (left) and sulfur (right) in the samples.

Bile X-glucuronide) agar and with Baird Parker were prepared for *E. coli*. and *S. gallinarum*, respectively. The bacterial suspension was prepared by adding bacteria from an inoculated colony cultured on agar to a physiological solution. The prepared inoculum concentration was 1.5×10^8 CFU/mL. The concentration was measured using a nephelometer (according to the McFarland standard of 0.5). The inoculum (1 mL) was spread over the agar in the Petri dish, and then, the nanofibrous material was added. Two replicates were prepared for each material and bacterial culture. The Petri dishes were placed in an incubator and incubated for 24 h at 37 °C.

2.10. Statistics. Data were evaluated using GraphPad Prism 7.05 (GraphPad Software, USA). All data were first tested for normality using the Shapiro–Wilk test, which is recommended for smaller sample sizes. The parametric *t*-test and nonparametric *t*-test (Mann–Whitney test) were chosen for pairwise comparison of groups. The ANOVA test with the Bonferroni correction with a significance level of $p \geq 0.001$ was used for parametric comparison of multiple groups. The Kruskal–Wallis (nonparametric ANOVA) test was used for nonparametric group comparisons. Values are given as the mean \pm standard deviation.

3. RESULTS

3.1. Productivity and Morphology. A total of six nanofibrous layers were prepared by needleless electrospinning; five with an incorporated antibiotic GS (1, 3, 5, 7.5, and 10%) and one control without the antibiotics. The materials are further denoted in the text as PCL (16% PCL without GS), PCL/1%GS (16% PCL with the addition of 1% GS), PCL/3%GS (16% PCL with the addition of 3% GS), PCL/5%GS (16% PCL with the addition of 5% GS), PCL/7.5%GS (16% PCL with the addition of 7.5% GS), and PCL/10%GS (16% PCL with the addition of 10% GS). The fabrication parameters are listed in Table 1. During the electrospinning of PCL/10% GS, the rewinding speed (the speed of a moving substrate, i.e., spunbond) was the lowest one, leading to slow and inefficient deposition of the nanofibers and inhomogeneities in the final PCL/10%GS material (visible mainly during macroscopical visual evaluation, data not shown). The antibiotic concentration of 10% GS can

thus be considered as the limit concentration for the chosen electrospinning method.

Figure 2 reveals SEM images of nanofibrous layers before and after sterilization. The morphology is characteristic of the biodegradable polycaprolactone, which is consistent with previously published studies.^{13,14} The final nanofibrous layers consist of both micro- and nanofibers, leading to large SD and outliers. The sterilization with ethylene oxide did not destroy or influence the fiber occurrence and morphology, and no degradation products or broken fibers were observed. Most of the materials had an average fiber diameter in the range of 280 to 380 nm. The largest fiber diameter was observed on the pure PCL material without an antibiotic (383 ± 240 nm), and vice versa the lowest fiber diameter was observed on PCL/7.5%GS (282 ± 200 nm).

3.2. Chemical Structure and Composition. **3.2.1. Elemental Analysis.** The amounts of nitrogen and sulfur elements were monitored, as the antibiotic gentamicin sulfate contains amine groups ($-\text{NH}_2$) and sulfates, which are formed by removing hydrogens from sulfuric acid. Figure 3 (left) shows the measured mass percent nitrogen content. As expected, a growing trend can be seen during elemental analysis, where the measured nitrogen content increases with a higher concentration of antibiotics in the material. This trend is also confirmed in the measurement of the sulfur content in Figure 3. The deviations between the measurements can be caused by sample moisture or residual solvent, which affects the measurement outcomes.

3.3. Contact Angle. Wettability (contact angle) was measured using a sessile drop as part of the evaluation of the surface properties of the materials (which are essential for cell adhesion, especially in the first seconds). The interactions with PBS, DIW, and AL were observed for both sterile and nonsterile materials, and the results were recorded over time (see Figure 4A–C). Although the contact angles did not differ significantly in the first second after drop deposition, the drop (of all test liquids) was gradually absorbed into the nanofibrous planar layers. As the antibiotic content in the nanofibers increased, the time needed to absorb the entire drop was prolonged. The different dynamics of soaking for sterile and nonsterile materials was also monitored (Figure 4D–F). It was observed that materials after sterilization had a slower course of wetting. The mean absorption time of the whole drop was

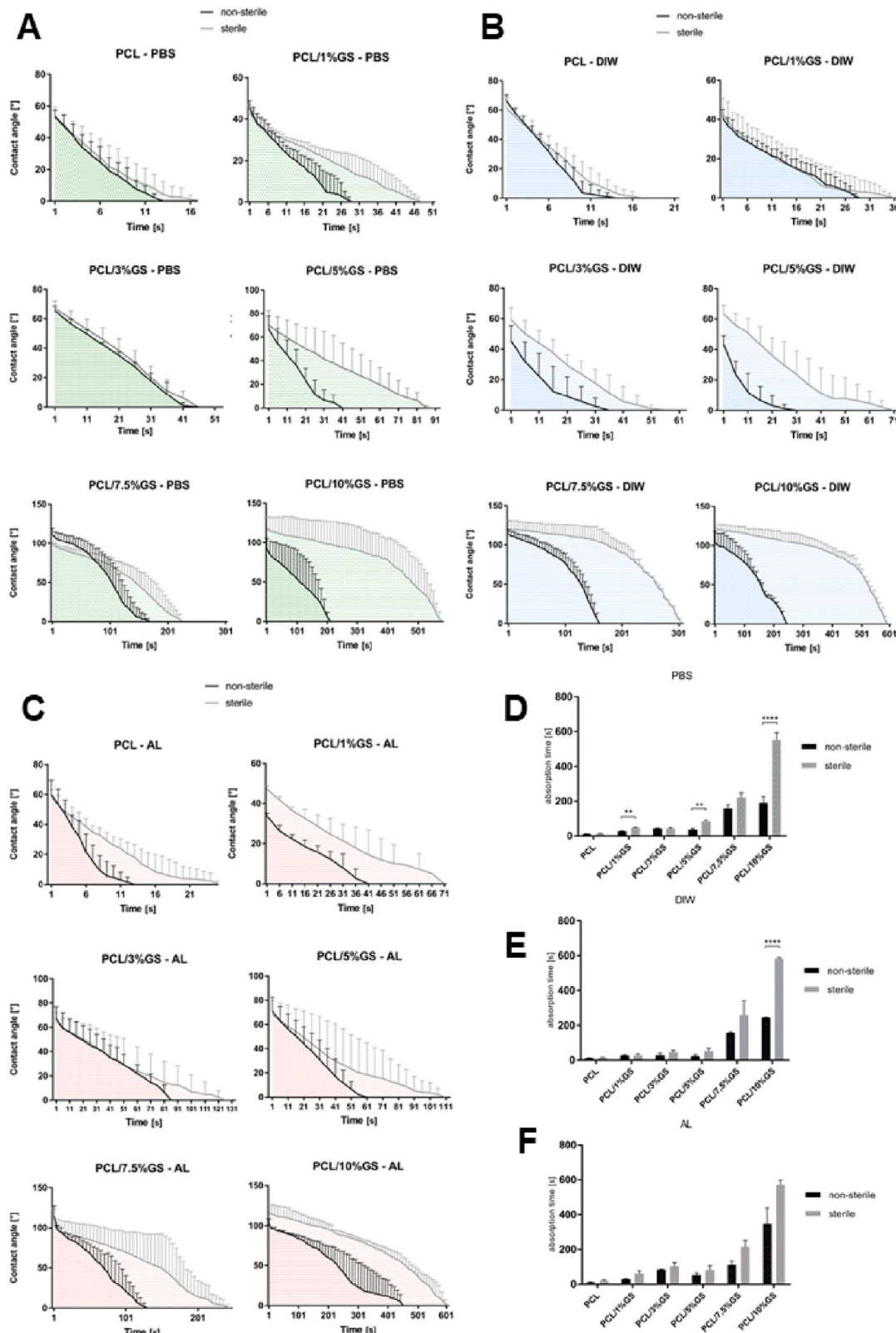


Figure 4. Change of the contact angle (sessile drop technique) over the contact angle over time. A drop of test liquids PBS (A), DIW (B), and AL (C) is gradually absorbed into the nanofibers. As the GS content increases, absorption slows down, and sterile and nonsterile materials show different trends. The absorption time was calculated and is shown for PBS (D), DIW (E), and AL (F) leading to statistically significant differences, especially between nonsterile and sterile PCL/10%GS.

evaluated, and it was shown that there were statistically significant differences between some materials (comparing sterile versus nonsterile).

3.4. Absorption. The percentage absorption (uptake) of fluids (PBS, DIW, and AL) and the change in weight of the materials were evaluated according to eqs 1 and 2. The

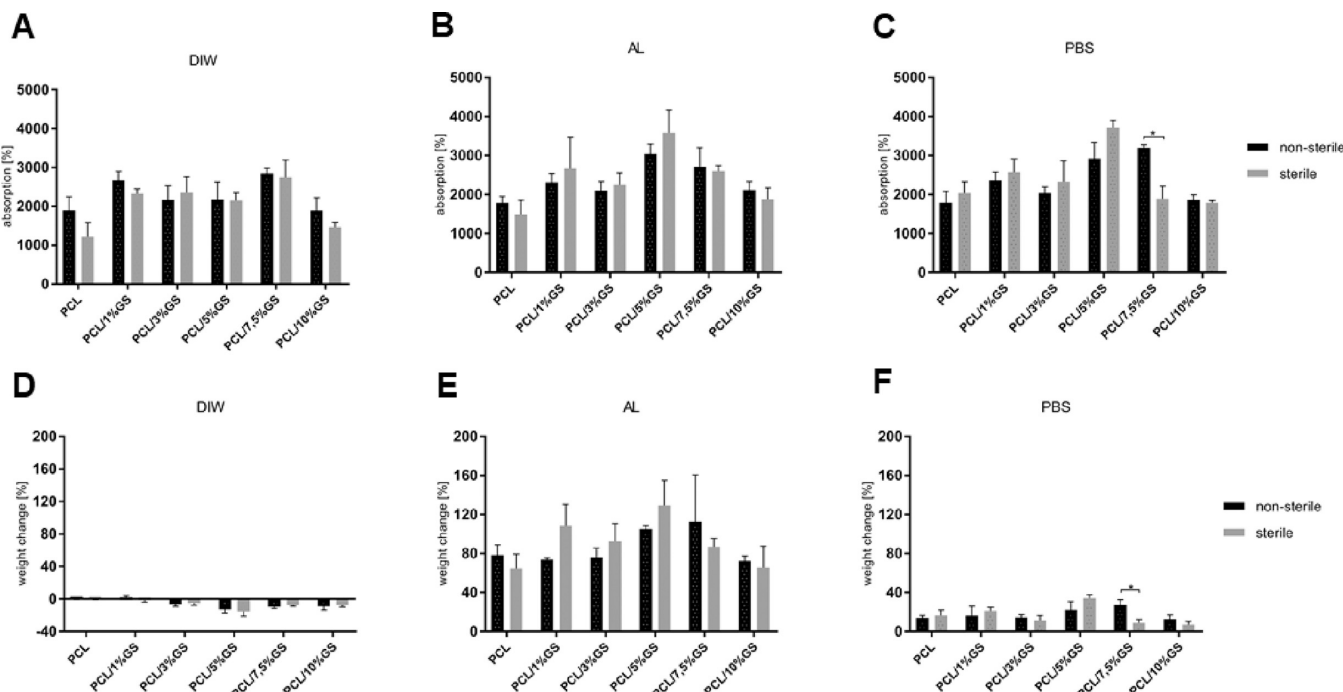


Figure 5. Absorption capacities of developed materials with DIW (A), AL (B), and PBS (C). For the weight change of nanomaterials, the materials were in direct contact with test fluids for 24 h. The weight change shows the difference before and after testing (after drying). The weight change of the materials after contact with test fluids was calculated, leading to the weight loss due to soluble antibiotics in the layers after testing with DIW (D). The weight gain occurred after contact with AL and PBS (E,F).

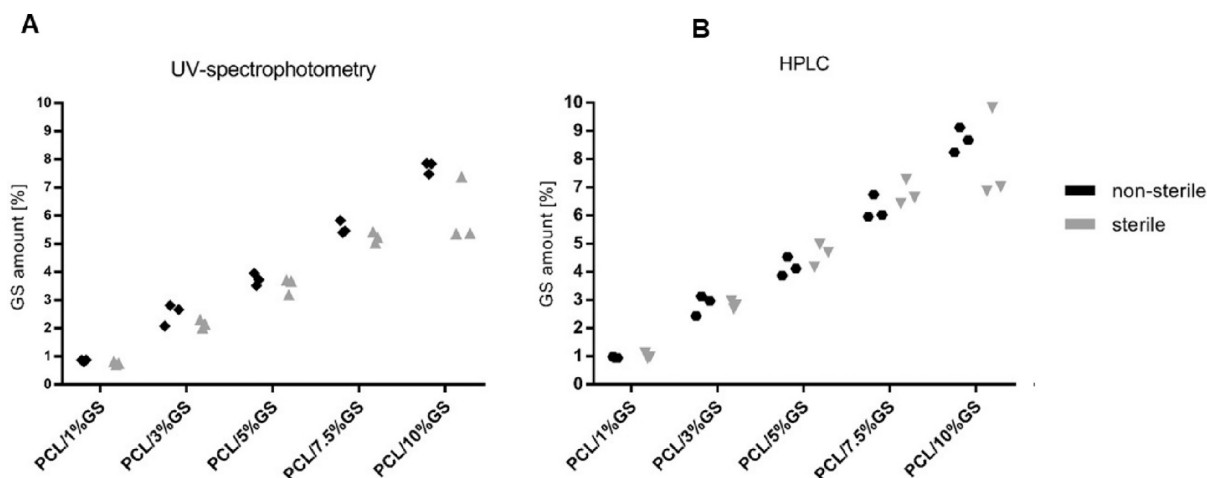


Figure 6. Measured amount of GS in the nanofibrous materials via UV spectrophotometry (A) and HPLC (B); $\lambda = 570$ nm.

materials were able to absorb the test fluids, as can be seen in Figure 5A–C. The highest absorption values were shown by the material nonsterile PCL/7.5%GS with $2846 \pm 133\%$ for DIW, sterile PCL/5%GS with $3583 \pm 584\%$ for AL, and sterile PCL/5%GS with $3710 \pm 187\%$ for PBS. Together with absorption, the change in weight of the materials after drying was evaluated. The materials that were in contact with distilled water exhibited a loss of weight (Figure 5D) since the antibiotic GS is soluble in water. Therefore, the decrease in weight was observed due to the dissolution and release of the antibiotic into the aqueous environment. After contact with PBS and the simulated intestinal fluid, a weight gain occurred (Figure 5E,F). This phenomenon was expected since the crystalline substances from PBS and AL can be easily captured in the nanofibrous meshes. The important finding here is that

the materials can absorb simulated body fluids and that drying occurs slowly with weight changes. This could be positive when applying the material, where any leakage of bowel contents could be captured and absorbed by the material.

3.5. UV Spectrophotometry and HPLC Chromatography. The amount of GS in the nanofibers is depicted in Figure 6A, showing a graph with the results of measurements on a UV spectrophotometer. The content of the GS antibiotics in the nanofibrous layers was detected by measuring the intensity of the purple gentamicin–ninhydrin complex. Both nonsterile and sterile samples were measured. The graph shows that the measured GS antibiotic content increases with higher GS concentrations in the layers. The measured content is lower than in the polymer solutions, which was expected since there are natural transfer losses during electrospinning (e.g.,

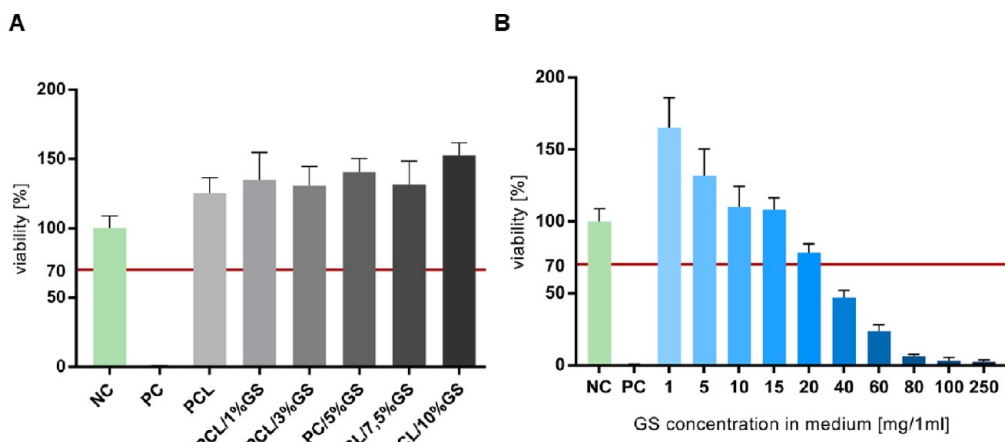


Figure 7. Graph of cytocompatibility of the developed and tested materials; PC and NC stand for positive (cytotoxic) and negative (cytocompatible) controls, respectively (A). Cytocompatibility of pure GS in the cell media. The cytotoxic concentration found (20 mg/1 mL) is the limit of cytocompatibility of GS in DMEM cell media (B).

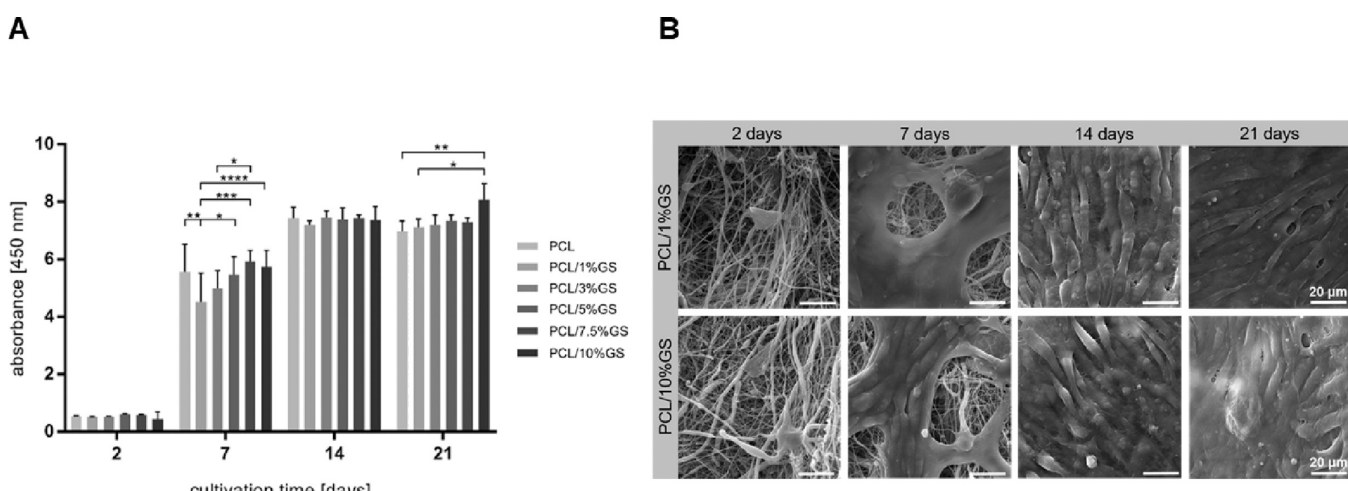


Figure 8. Metabolic activity of 3T3 mouse fibroblasts on the nanofibrous scaffold with different concentrations of GS. All tested materials supported cell growth within the observed time period (A). Example of spread cells on materials taken via SEM, with a scale bar of 50 μ m. The cells are spread across the material with no preferential direction after 7 days. The 100% confluence is reached after 21 days; the fibrous surface is fully grown with cells (B).

the minimal amount of the solution remains in the cartridge or on the steel wire). Figure 6 also reveals and supports the previously mentioned inhomogeneity of the PCL/10% GS material; the measured values are lower for sterile materials. This observation may be due to the uneven distribution of GS in the nanofibrous layer due to the large amount of GS in the spinning solution leading to nonuniform electrospinning with a low transfer rate of GS into the final nanofibrous layer. The results of the HPLC method correspond to the results of UV spectrophotometry (see Figure 6B); GS is present in the materials at the expected ratio. As with UV spectrophotometry, the lower values with higher variability were measured for the sterile PCL/10%GS material due to the inhomogeneity rather than the sterilization process.

3.6. In Vitro Testing. The cytotoxicity of prepared materials and the GS antibiotic dissolved in the cell media at different concentrations was evaluated. In Figure 7A, the percentage viability graph can be seen for individual material extracts. The red line indicates the limit value of cytotoxicity (according to ISO 10993:5) in the diagram. The values of the materials were assessed against the negative control (NC),

which represents the cells in the DMEM medium and thus indicates 100% viability. The positive control (PC) stands for the cells in a cytotoxic solution of medium and Triton-X. The graph in Figure 7A shows that all prepared fibrous materials are cytocompatible. Figure 7B shows a diagram of cell viability for individual concentrations of GS in a DMEM medium. The limit cytotoxic concentration was found, namely, 20 mg of GS in DMEM. The solutions with a higher content of GS are not appropriate for cell use. However, the most important finding of this trial is that the chosen concentrations of GS in the electrospinning polymer solutions are nontoxic since the maximum concentration of GS in our solutions is 16 mg per 1 mL of electrospinning solution (for PCL/10%GS).

Cell adhesion and proliferation were evaluated during 21 days of in vitro cell testing. In Figure 8A, the metabolic activity graph is evaluated using the CCK-8 metabolic test. During the first testing day (day 2), the measured absorbance reached only small values; however, within 7 days, the metabolic activity of the cells increased significantly. After 14 days, enhanced cell viability can be observed with no significant changes within the tested materials. The measured values did not increase for the

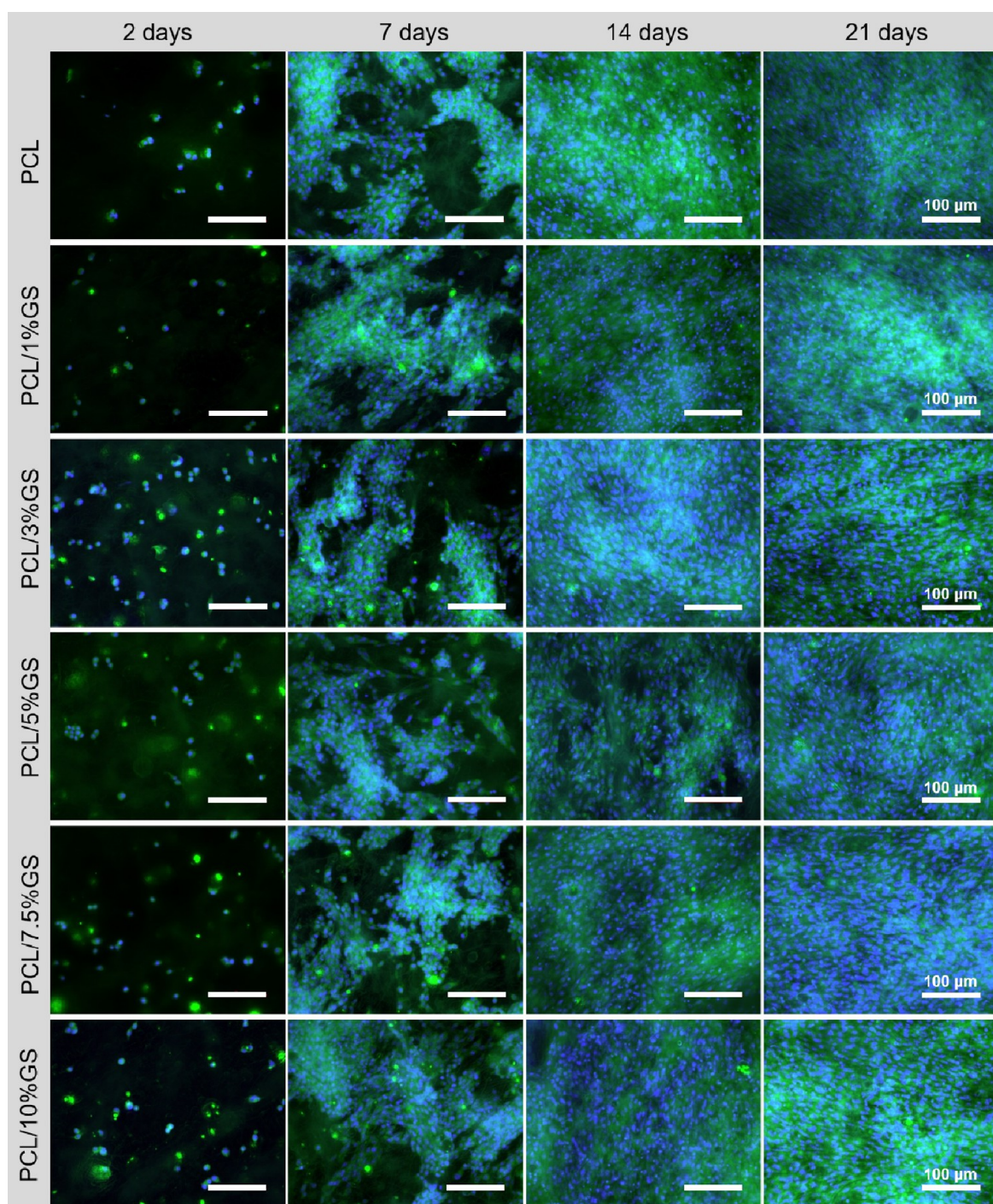


Figure 9. Fluorescence microscopy images of fibroblasts cultured on PCL nanofibrous scaffolds with different antibiotic concentrations. The images show the cell proliferation after 4, 7, 14, and 21 days of cultivation with nanofibers; scale bar of 100 μm .

last testing day (21st day) except for PCL/10%GS. The phenomena may be explained with the materials being fully grown with cells after 21 days of cultivation. The cells reached over 100% confluence after 14 days followed by inefficient nutrition from the medium, leading to decreased viability. The 100% confluency is supported via obtained SEM images of cells on the material's surface, as can be seen on Figure 8B. Only two materials (with the lowest and highest concentrations of GS in PCL) are shown as an example. Figure 9 shows the fluorescence microscopy images during the cultivation period. Cell nuclei are stained by DAPI (resulting

in a blue color), while the cytoskeleton is visible due to the phalloidin–FITC complex (green color). During the first testing day, only the single round cells were found, which started to irregularly spread across the nanofibrous surface, as can be seen in Figure 9 on day 7. The cells gradually reached 100% confluence of the material's surface and started to overgrow during the last testing day. This observation corresponds with the previously mentioned results about metabolic activity (a slight decrease during the 21st testing day) and with the SEM images of cells.

3.7. Antibacterial Properties. The antibacterial properties were evaluated by direct contact of materials with *Escherichia coli* and *Staphylococcus gallinarum*. The results support the expected antibacterial behavior of prepared nanofibrous layers. The inhibition of bacteria colony growth was measured, further supporting the hypothesis regarding the antibacterial effect of the developed fibers. In Table 2, the

Table 2. Measured Inhibition Zones (mm) in the Form of Average \pm SD

material	inhibition zone (<i>E. coli</i>)	inhibition zone (<i>S. gallinarum</i>)
PCL	0 \pm 0	0 \pm 0
PCL/1%GS	6.4 \pm 0.5	12.3 \pm 0.5
PCL/3%GS	7.6 \pm 0.1	12.5 \pm 0.4
PCL/5%GS	7.9 \pm 0.7	12.8 \pm 0.5
PCL/7.5%GS	8.7 \pm 0.8	13.0 \pm 0.9
PCL/10%GS	10.0 \pm 0.6	15.5 \pm 0.5

zones' diameters are increasing with the growing concentration of the antibiotics in the materials. The examples of the inhibition zones are evident in Figure 10 where three materials were selected for demonstration of the results (namely, PCL, PCL/1%GS, and PCL/10%GS). As expected, no changes appeared in the Petri dish with the pure PCL material (A and D) regardless of the bacteria used; the bacteria grew through the material. For the antibiotic-containing materials, the size of the inhibition zones increased with a growing GS concentration in the layers, further supporting the hypothesis regarding the antibacterial effect of the developed fibers.

4. DISCUSSION

This study describes the development and testing of planar nanofibrous materials with antibacterial activity. There are other studies introducing antibacterial nanofibers for biomedical applications.^{15–18} However, most of the reported approaches are based on needle electrospinning, which does not allow for large-scale and homogeneous production of

nanofibers, which is crucial for introducing the product to the market and clinical practice. Moreover, previously published studies usually do not consider the effect of sterilization on the final properties of the materials. We believe that the lack of these findings leads to significant roadblocks in translating research outcomes into routine clinical practice.

The present article builds on our previous research and development in nanofibrous materials for covering intestinal anastomoses.^{9–11} In this follow-up study, we report findings regarding the possible prevention of postoperative complications in gastrointestinal surgery using local antibacterial coverage of intestinal anastomosis. However, the knowledge gained is not limited only to the presented use case and can be readily translated to other medical areas. Our material consists of biocompatible and biodegradable poly- ϵ -caprolactone; the biocompatibility was previously proven in vivo.⁹ Gentamicin sulfate was chosen as the antibacterial agent. The main reason behind choosing GS is its activity against bacteria (e.g., *Pseudomonas*, *Bacillus*, and *Clostridium*) that produce the enzyme collagenase, which causes collagen breakdown in the newly formed tissue leading to tissue degradation and slower healing.^{19,20}

The morphology of the fibers was evaluated via scanning electron microscopy. Based on the SEM images, incorporating the antibiotic into the nanofibrous layers did not affect the morphology of the materials. The average fiber diameter was in the range of 280 to 380 nm. The nonsterile PCL material without antibiotics had the largest fiber diameter (383 \pm 239 nm), while the lowest fiber diameter was observed on the nonsterile PCL/7.5%GS with the value of 282 \pm 201 nm. The diameter of the nanofibers can affect the release rate of the incorporated substance, as well as the mechanical properties of the nanofibers. As reported in the study by Alharbi et al., fibers with a smaller diameter have higher fiber stiffness compared to fibers with larger diameters. However, this observation mainly concerns fibers below 100 nm; fibers with diameters higher than 100 nm have their moduli close to the value of bulk PCL.²¹ The diameters are similar to nanofibrous materials

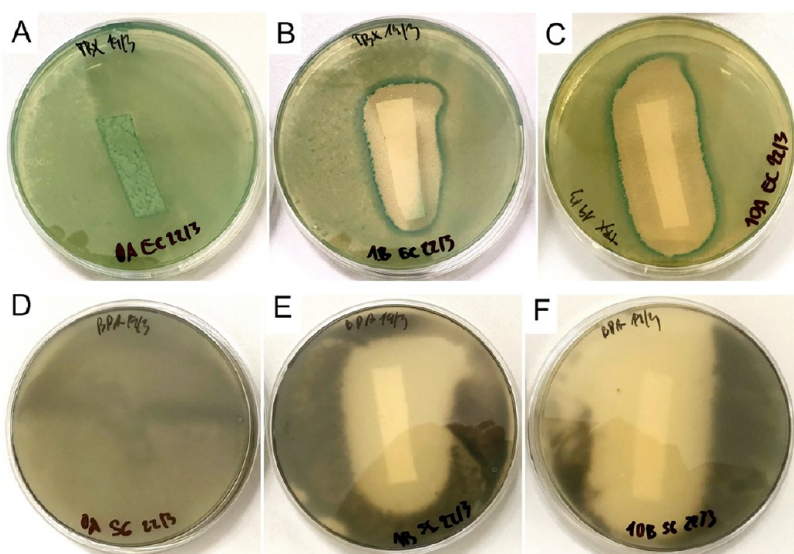


Figure 10. (Above) Petri dishes with TBX (Tryptone Bile X-glucuronide) agar and *Escherichia coli* bacterium inoculum; 10 \times 40 mm materials were inserted, and after 24 h, the zones of inhibition were monitored; (A) PCL; (B) PCL/1%GS; (C) PCL/10%GS. (Under) Petri dishes with Baird Parker agar and inoculum bacteria *Staphylococcus gallinarum*, where 10 \times 40 mm materials have been inserted for 24 h, and then, the halo zones were monitored; (D) PCL; (E) PCL/1%GS; (F) PCL/10%GS.

already tested *in vivo* in the study by Rosendorf et al., where PCL nanofibrous layers had a fiber diameter of 385 ± 239 nm.¹¹ The fabrication process was optimized to reach the material's basis weight of 10 g/m^2 since it was previously found that a lower basis weight supports tissue healing and fast resorption *in vivo*.¹⁰

In this study, the contact angle was measured as a function of time. The wettability value of the scaffold's surface affects both the release of the active substances, especially in the case of water-soluble GS, as well as the adhesion of cell cultures, as has already been proven by Bacakova et al. The moderately hydrophilic materials create the most adequate surfaces for cell adhesion and growth since the cell adhesion-mediating molecules tend to adsorb to materials with high surface energy.²² It was shown that although the materials appear nonwetting in the first seconds, over time, the test liquids (in this case DIW, AL, and PBS) fully soak into the nanofibrous material. This fact is an important observation and points out that the presentation of the contact angle only immediately after drop deposition on the material does not necessarily provide a full, accurate representation of the actual properties of the material. The length of soaking varied when comparing materials with different GS contents, and we observed that the time needed to soak a drop increased with a growing antibiotic content. It is also worth noting that we observed different dynamics of drop soaking between sterile and nonsterile materials. Based on the data obtained, the average time of complete absorption of the test drops was monitored, and it was shown that in a number of cases, there were statistically significant differences in absorption. On the other hand, it should be noted that the most significant differences occurred with the PCL/10%GS material, which was evaluated as the least suitable due to the uneven distribution of the antibiotic in the material, which can affect the absorption measurement.

The presence of antibiotics was confirmed by multiple methods. The elemental analysis revealed that the measured percentage of nitrogen and sulfur was growing with an increasing amount of GS in the fibers as expected. UV spectrophotometry and high-performance liquid chromatography were used to directly assess the amount of GS in the materials; the gentamicin–ninhydrin complex was measured. Ninhydrin reacts with the primary and secondary amino groups in the structure of GS, forming a violet-colored complex. UV spectrophotometry results confirm the increasing trend of the GS content with an increasing GS concentration in the layers. In this work, the GS quantification methodology was optimized compared with the current literature. The quantification of GS by UV spectrophotometry (gentamicin–ninhydrin method) was already carried out in other publications at 418 nm.^{4,23} However, the previously chosen methods are not appropriate for these complexes. For example, in Pisani et al.'s work, the amount of GS in fibers was measured spectrometrically after derivatization to a purple product at 418 nm, at which absorption occurs not only in the GS but also in the agent, resulting in a significant influence on the readout. Therefore, a different wavelength (570 nm) was used in our study.

The cytocompatibility of all tested materials was proven; nanofibrous materials with different concentrations of GS were already tested by Abdul Khodir et al., and no cytotoxicity was observed as well.⁸ The pure GS powder in cell media was also tested, and the concentration of 20 mg GS/1 mL of media was found to be on the cytotoxic threshold. This trial proves that

not only the final products but also the chosen concentrations of GS in the polymeric solutions for electrospinning are cytocompatible. The antibiotic presence in fibers did not affect cell adhesion and proliferation according to the CCK-8 metabolic test or visualization of the cell morphology (via SEM and fluorescence microscopy). The cells gradually grew over the entire nanofibrous surface with no significant differences within the tested materials.

Microbial tests confirmed antibacterial effects on both Gram-positive and Gram-negative bacteria. The release of the antibiotics occurred within 24 h, and the inhibition zones were expectedly more pronounced with a growing concentration of the antibiotic in the layers. The control material (pure PCL) had no antibacterial effects, and bacteria grew over it. Most previously mentioned publications report a rapid initial release.^{4,7,8} Some publications say that up to 80% of the antibiotic GS was released within 24 h. To prolong the release or to ensure constant drug delivery, the literature recommends choosing a different structure of the nanofiber scaffold, e.g., core/sheath fibers, layering of nanofibrous layers on top of each other (sandwich structure), use of emulsion spinning, or encapsulation of the substance in a liposome.^{17,24,25} However, these approaches are difficult to translate into industrial production and are beyond the scope of this study.

The presented data were measured on nonsterile and sterile materials with ethylene oxide. There are other methods of sterilizing medical products such as steam sterilization, γ radiation, ozone radiation, plasma sterilization, and others.²⁶ Ethylene oxide was chosen due to its low sterilization temperature (37°C) and because the layers contained active substances that would be leached out using wet sterilization methods. The PCL polymer has a low melting point; thus, at higher temperatures, melting or degradation would occur.

The effect of ethylene oxide sterilization of pure PCL nanofibrous materials is described in a previous publication by Horakova et al. The publication reports insignificant changes in the sterilized materials' morphology, chemical composition, degradation rate, or mechanical properties. However, they show slower cell proliferation after ethylene oxide sterilization compared to other techniques.^{27,28} Friess and Schlapp tested the GS structural changes after sterilization. It was reported that after sterilizing GS with ethylene oxide, there were small changes in the molecule's structure confirmed by nuclear magnetic resonance spectroscopy. However, the changes in the structure were not crucial for the antibacterial effects.²⁹ In a more recent study, the sterile films from PLGA/pullulan with incorporated GS were tested, and the films had an expected antibacterial effect even after sterilization.³⁰ The previously mentioned results are in agreement with our findings. In our study, it was verified that the structure and antibacterial properties of GS were preserved. Sterilization did not cause any changes in the functionality of the material; however, as mentioned above, there was a different behavior in the absorption of the test fluids.

Elucidating the differences between sterile and nonsterile materials would require further intensive characterization of changes in surface properties; however, it seems that it could also be related to slower cell adhesion on ethylene oxide-sterilized materials, as already observed in ref 23. The wettability of the surface is one of the essential properties of the scaffold, which affects the adhesion of proteins (*in vitro* or *in vivo*) and, subsequently, of cells in the first seconds after

contact with the material. Another suitable method for GS sterilization could be γ radiation, as mentioned in ref 31.

5. CONCLUSIONS

In this study, we follow our long-term research in developing nanofibrous planar materials for sealing and fortifying gastrointestinal anastomoses. However, we believe that our findings have an increased impact since the developed antibacterial scaffold is suitable for more biomedical applications. In our study, the preparation of antibacterial materials was optimized on a semi-industrial scale. The nanofibers based on biodegradable polycaprolactone were chosen as the carrier matrix of gentamicin sulfate, both specifically on the basis of previous *in vivo* research and also due to the general properties of nanofibers (large surface area, resemblance to intercellular mass, etc.), indicating the suitability of nanofibrous structures for drug delivery systems. A limit concentration of the GS content in polymer solutions was found; the antibiotic content of around 10% relative to the dry matter is the processing limit, as shown by the productivity and also revealed by the measurement results. The real (measured) content of the antibiotics in the layers was consistent for all samples except PCL/10%GS, where the values were scattered. We do not attribute this phenomenon to the effect of sterilization but to the inhomogeneous distribution of the active substance in the layer, even though the effect of sterilization with ethylene oxide itself was monitored. The properties of the nanofibrous materials were observed after contact with distilled water and simulated body fluids. It was observed that all materials are cytocompatible, support cell growth, and at the same time show sufficient antibacterial properties and can thus be further tested for medical applications.

■ ASSOCIATED CONTENT

Data Availability Statement

All data included in the article.

■ AUTHOR INFORMATION

Corresponding Author

Marketa Klicova — Department of Nonwovens and Nanofibrous Materials, Faculty of Textile Engineering, Technical University of Liberec, Liberec 461 17, Czech Republic; orcid.org/0000-0002-0942-6126; Email: marketa.klicova@tul.cz

Authors

Senta Mullerova — Department of Nonwovens and Nanofibrous Materials, Faculty of Textile Engineering, Technical University of Liberec, Liberec 461 17, Czech Republic

Jachym Rosendorf — Biomedical Center, Faculty of Medicine in Pilsen, Charles University, Plzen 323 00, Czech Republic; orcid.org/0000-0003-2125-0685

Andrea Klapstova — Department of Nonwovens and Nanofibrous Materials, Faculty of Textile Engineering, Technical University of Liberec, Liberec 461 17, Czech Republic

Radek Jirkovec — Department of Nonwovens and Nanofibrous Materials, Faculty of Textile Engineering, Technical University of Liberec, Liberec 461 17, Czech Republic; orcid.org/0000-0001-7133-4452

Jakub Erben — Department of Nonwovens and Nanofibrous Materials, Faculty of Textile Engineering, Technical

University of Liberec, Liberec 461 17, Czech Republic;

orcid.org/0000-0001-9856-1604

Michaela Petrzilkova — Faculty of Mechatronics, Informatics and Interdisciplinary Studies, Institute of New Technologies and Applied Informatics, Liberec 461 17, Czech Republic

Hedvika Raabová — Faculty of Pharmacy, The Department of Analytical Chemistry, Charles University, Hradec Kralove 500 05, Czech Republic

Dalibor Satinský — Faculty of Pharmacy, The Department of Analytical Chemistry, Charles University, Hradec Kralove 500 05, Czech Republic; orcid.org/0000-0002-4057-9542

Jana Melicherikova — The Institute for Nanomaterials, Advanced Technologies and Innovation, Technical University of Liberec, Liberec 460 01, Czech Republic

Richard Palek — Biomedical Center, Faculty of Medicine in Pilsen, Charles University, Plzen 323 00, Czech Republic

Vaclav Liska — Biomedical Center, Faculty of Medicine in Pilsen, Charles University, Plzen 323 00, Czech Republic

Jana Horakova — Department of Nonwovens and Nanofibrous Materials, Faculty of Textile Engineering, Technical University of Liberec, Liberec 461 17, Czech Republic

Complete contact information is available at:

<https://pubs.acs.org/10.1021/acsomega.3c05924>

Author Contributions

M.K. and J.R. performed conceptualization; S.M., J.M., H.R., and D. \check{S} . performed methodologies; M.K., J.H., and D. \check{S} . performed the investigation; M.K. and S.M. acquired resources; R.J., R.P., and J.E. performed data curation; M.K. performed original draft preparation; S.M., A.K., R.J., and J.E. performed review and editing of the manuscript; A.K. performed visualization; J.H. and V.L. performed supervision, project administration, and funding acquisition. All authors have read and agreed to the published version of the manuscript.

Notes

The authors declare no competing financial interest.

Not applicable. The study did not require ethical approval.

Not applicable. The study does not involve human patients.

■ ACKNOWLEDGMENTS

This research was funded by the Czech Health Research Council project AZV NU20J-08-00009 prevention of intestinal anastomotic leakage and postoperative adhesions by using nanofibrous biodegradable materials.

■ REFERENCES

- (1) Luraghi, A.; Peri, F.; Moroni, L. Electrospinning for Drug Delivery Applications: A Review. *J. Controlled Release* **2021**, *334*, 463–484.
- (2) Gunay, M. S.; Ozer, A. Y.; Chalon, S. Drug Delivery Systems for Imaging and Therapy of Parkinson's Disease. *Curr. Neuropharmacol.* **2016**, *14* (4), 376–391.
- (3) Dahlin, R. L.; Kasper, F. K.; Mikos, A. G. Polymeric Nanofibers in Tissue Engineering. *Tissue Eng. Part B* **2011**, *17* (5), 349–364.
- (4) Pisani, S.; Dorati, R.; Chiesa, E.; Genta, I.; Modena, T.; Bruni, G.; Grisoli, P.; Conti, B. Release Profile of Gentamicin Sulfate from Polylactide-Co-Polycaprolactone Electrospun Nanofiber Matrices. *Pharmaceutics* **2019**, *11* (4), E161.
- (5) Ceylan, M.; Yang, S.-Y.; Asmatulu, R. Effects of Gentamicin-Loaded PCL Nanofibers on Growth of Gram Positive and Gram Negative Bacteria. *Eur. J. Appl. Microbiol. Biotechnol.* **2017**, *5*, 40–51.

- (6) Sirc, J.; Kubinova, S.; Hobzova, R.; Stranska, D.; Kozlik, P.; Bosakova, Z.; Marekova, D.; Holan, V.; Sykova, E.; Michalek, J. Controlled Gentamicin Release from Multi-Layered Electrospun Nanofibrous Structures of Various Thicknesses. *Int. J. Nanomed.* **2012**, *7*, 5315–5325.
- (7) Coimbra, P.; Freitas, J. P.; Gonçalves, T.; Gil, M. H.; Figueiredo, M. Preparation of Gentamicin Sulfate Eluting Fiber Mats by Emulsion and by Suspension Electrospinning. *Mater. Sci. Eng.: C* **2019**, *94*, 86–93.
- (8) Abdul Khodir, W. K. W.; Abdul Razak, A. H.; Ng, M. H.; Guarino, V.; Susanti, D. Encapsulation and Characterization of Gentamicin Sulfate in the Collagen Added Electrospun Nanofibers for Skin Regeneration. *J. Funct. Biomater.* **2018**, *9* (2), E36.
- (9) Rosendorf, J.; Horakova, J.; Klicova, M.; Palek, R.; Cervenkova, L.; Kural, T.; Hosek, P.; Kriz, T.; Tegl, V.; Moulisova, V.; Tonar, Z.; Treska, V.; Lukas, D.; Liska, V. Experimental Fortification of Intestinal Anastomoses with Nanofibrous Materials in a Large Animal Model. *Sci. Rep.* **2020**, *10* (1), 1–12.
- (10) Rosendorf, J.; Klicova, M.; Cervenkova, L.; Horakova, J.; Klapstova, A.; Hosek, P.; Palek, R.; Sevcik, J.; Polak, R.; Treska, V.; Chvojka, J.; Liska, V. Reinforcement of Colonic Anastomosis with Improved Ultrafine Nanofibrous Patch: Experiment on Pig. *Biomedicines* **2021**, *9* (2), 102.
- (11) Rosendorf, J.; Klicova, M.; Cervenkova, L.; Palek, R.; Horakova, J.; Klapstova, A.; Hosek, P.; Moulisova, V.; Bednar, L.; Tegl, V.; Brzon, O.; Tonar, Z.; Treska, V.; Lukas, D.; Liska, V. Double-Layered Nanofibrous Patch for Prevention of Anastomotic Leakage and Peritoneal Adhesions, Experimental Study. *In Vivo* **2021**, *35* (2), 731–741.
- (12) Choi, E. J.; Son, B.; Hwang, T. S.; Hwang, E.-H. Increase of Degradation and Water Uptake Rate Using Electrospun Star-Shaped Poly(d,L-Lactide) Nanofiber. *J. Ind. Eng. Chem.* **2011**, *17* (4), 691–695.
- (13) Kamath, S. M.; Sridhar, K.; Jaison, D.; Gopinath, V.; Ibrahim, B. K. M.; Gupta, N.; Sundaram, A.; Sivaperumal, P.; Padmapriya, S.; Patil, S. S. Fabrication of Tri-Layered Electrospun Polycaprolactone Mats with Improved Sustained Drug Release Profile. *Sci. Rep.* **2020**, *10* (1), 18179.
- (14) Klicova, M.; Klapstova, A.; Chvojka, J.; Koprivova, B.; Jencova, V.; Horakova, J. Novel Double-Layered Planar Scaffold Combining Electrospun PCL Fibers and PVA Hydrogels with High Shape Integrity and Water Stability. *Mater. Lett.* **2020**, *263*, No. 127281.
- (15) Liu, Q.; Ouyang, W.-C.; Zhou, X.-H.; Jin, T.; Wu, Z.-W. Antibacterial Activity and Drug Loading of Moxifloxacin-Loaded Poly(Vinyl Alcohol)/Chitosan Electrospun Nanofibers. *Front. Mater.* **2021**, *82*, No. 643428, DOI: [10.3389/fmats.2021.643428](https://doi.org/10.3389/fmats.2021.643428).
- (16) Wei, Z.; Wang, L.; Zhang, S.; Chen, T.; Yang, J.; Long, S.; Wang, X. Electrospun Antibacterial Nanofibers for Wound Dressings and Tissue Medicinal Fields: A Review. *J. Innov. Opt. Health Sci.* **2020**, *13* (05), 2030012.
- (17) Gao, Y.; Truong, Y. B.; Zhu, Y.; Kyratzis, I. L. Electrospun Antibacterial Nanofibers: Production, Activity, and in Vivo Applications. *J. Appl. Polym. Sci.* **2014**, *131* (18), 9041 DOI: [10.1002/app.40797](https://doi.org/10.1002/app.40797).
- (18) Ali, I. H.; Ouf, A.; Elshishiny, F.; Taskin, M. B.; Song, J.; Dong, M.; Chen, M.; Siam, R.; Mamdouh, W. Antimicrobial and Wound-Healing Activities of Graphene-Reinforced Electrospun Chitosan/Gelatin Nanofibrous Nanocomposite Scaffolds. *ACS Omega* **2022**, *7* (2), 1838–1850.
- (19) Scharday, H. M.; Rogers, S.; Schopf, S. K.; von Ahnen, T.; Wirth, U. Are Gut Bacteria Associated with the Development of Anastomotic Leaks? *Coloproctology* **2017**, *39* (2), 94–100.
- (20) Kadurugamuwa, J. L.; Clarke, A. J.; Beveridge, T. J. Surface Action of Gentamicin on Pseudomonas Aeruginosa. *J. Bacteriol.* **1993**, *175* (18), 5798–5805.
- (21) Alharbi, N.; Daraei, A.; Lee, H.; Guthold, M. The Effect of Molecular Weight and Fiber Diameter on the Mechanical Properties of Single, Electrospun PCL Nanofibers. *Mater. Today Commun.* **2023**, *35*, No. 105773.
- (22) Bacakova, L.; Filova, E.; Parizek, M.; Rum, T.; Svorcik, V. Modulation of Cell Adhesion, Proliferation and Differentiation on Materials Designed for Body Implants. *Biotechnol. Adv.* **2011**, *29* (6), 739–767.
- (23) Ismail, A. F. H.; Mohamed, F.; Rosli, L. M. M.; Shafri, M. A. M.; Haris, M. S.; Adina, A. B. Spectrophotometric Determination of Gentamicin Loaded PLGA Microparticles and Method Validation via Ninhydrin-Gentamicin Complex As A Rapid Quantification Approach. *J. Appl. Pharm. Sci.* **2016**, *6*, 007–014.
- (24) Kuang, G.; Zhang, Z.; Liu, S.; Zhou, D.; Lu, X.; Jing, X.; Huang, Y. Biphasic Drug Release from Electrospun Polyblend Nanofibers for Optimized Local Cancer Treatment. *Biomater. Sci.* **2018**, *6* (2), 324–331.
- (25) Kajdič, S.; Planinšek, O.; Gašperlin, M.; Kocbek, P. Electrospun Nanofibers for Customized Drug-Delivery Systems. *J. Drug Delivery Sci. Technol.* **2019**, *S1*, 672–681.
- (26) Mendes, G. C. C.; Brandão, T. R. S.; Silva, C. L. M. Ethylene Oxide Sterilization of Medical Devices: A Review. *Am. J. Infect. Control* **2007**, *35* (9), 574–581.
- (27) Horakova, J.; Mikes, P.; Saman, A.; Jencova, V.; Klapstova, A.; Svarcova, T.; Ackermann, M.; Novotny, V.; Suchy, T.; Lukas, D. The Effect of Ethylene Oxide Sterilization on Electrospun Vascular Grafts Made from Biodegradable Polyesters. *Mater. Sci. Eng. C* **2018**, *92*, 132–142.
- (28) Horakova, J.; Klicova, M.; Erben, J.; Klapstova, A.; Novotny, V.; Behalek, L.; Chvojka, J. Impact of Various Sterilization and Disinfection Techniques on Electrospun Poly- ϵ -Caprolactone. *ACS Omega* **2020**, *5* (15), 8885–8892.
- (29) Friess, W.; Schlapp, M. Sterilization of Gentamicin Containing Collagen/PLGA Microparticle Composites. *Eur. J. Pharm. Biopharm.* **2006**, *63* (2), 176–187.
- (30) Dhal, C.; Mishra, R. In Vitro and in Vivo Evaluation of Gentamicin Sulphate-Loaded PLGA Nanoparticle-Based Film for the Treatment of Surgical Site Infection. *Drug Delivery Transl. Res.* **2020**, *10* (4), 1032–1043.
- (31) Mullins, N. D.; Deadman, B. J.; Moynihan, H. A.; McCarthy, F. O.; Lawrence, S. E.; Thompson, J.; Maguire, A. R. The Impact of Storage Conditions upon Gentamicin Coated Antimicrobial Implants. *J. Pharm. Anal.* **2016**, *6* (6), 374–381.